PHILOSOPHICAL TRANSACTIONS OF THE ROYAL SOCIETY B BIOLOGICAL SCIENCES

Single–motor mechanics and models of the myosin motor

T. Yanagida, S. Esaki, A. Hikikoshi Iwane, Y. Inoue, A. Ishijima, K. Kitamura, H. Tanaka and M. Tokunaga

Phil. Trans. R. Soc. Lond. B 2000 **355**, 441-447
doi: 10.1098/rstb.2000.0585

THE ROYAL SOCIETY

Single-motor mechanics and models of the myosin motor

T. Yanagida[1,2,3*], S. Esaki[3], A. Hikikoshi Iwane[3], Y. Inoue[2], A. Ishijima[1], K. Kitamura[2], H. Tanaka[2] and M. Tokunaga[1]

[1]*Yanagida BioMotron Project, Exploratory Research for Advanced Technology, and* [2]*Single Molecule Process Project, International Cooperative Research Project, Japan Science and Technology Corporation, 2-4-14 Senba-Higashi, Mino, Osaka 562-0035, Japan* [3]*Department of Physiology I, Osaka University Medical School, 2-2 Yamadaoka, Suita, Osaka 565-0871, Japan*

Recent progress in single-molecule detection techniques is remarkable. These techniques have allowed the accurate determination of myosin-head-induced displacements and how mechanical cycles are coupled to ATP hydrolysis, by measuring individual mechanical events and chemical events of actomyosin directly at the single-molecule level. Here we review our recent work in which we have made detailed measurements of myosin step size and mechanochemical coupling, and propose a model of the myosin motor.

Keywords: Brownian motion; torsional strain; single-molecule imaging; single-molecule manipulation; lever-arm model; myosin step size

1. INTRODUCTION

Muscle contraction and a large part of other biological motions are propelled by a relative sliding between two kinds of filaments, consisting of actin and myosin molecules (Huxley & Niedergerke 1954; Huxley & Hanson 1954). The sliding movement is believed to result from cyclic interactions of a myosin head (S1) with an actin filament coupled to ATP hydrolysis (Huxley 1957). Structural and mechanical studies of muscle fibres have been performed extensively and a swinging cross-bridge model has been proposed to explain the mechanism of muscle contraction (Huxley 1969; Huxley & Simmons 1971), in which the myosin hauls an actin filament by swinging its head. This model, coupled to the kinetic pathway of ATP hydrolysis determined in solution (Lymn & Taylor 1971), has been widely used as a working hypothesis to analyse experimental data. Despite many investigations, however, direct evidence of the swinging cross-bridge model has not been obtained. Recently, investigations of the actomyosin motor have made rapid progress. The crystal structures of the actin monomer (Kabsch *et al.* 1990) and the myosin head (Rayment *et al.* 1993*a*) have been obtained, which have provided a structural framework for understanding the interaction between actin and the myosin head. Based on the conformational changes in the myosin head complexed with nucleotide analogues in crystals, a model, termed 'the lever-arm hypothesis' has been proposed, in which the structural change in the catalytic domain of a myosin head is magnified by a pivoting of the light-chain binding domain (*ca.* 10 nm long) acting as a lever arm (Rayment *et al.* 1993*b*). This is essentially the same as a variation of the original swinging cross-bridge model (Huxley 1974). The current model suggests that the displacement caused by pivoting the lever arm is *ca.* 6 nm (Cooke 1997).

Development of techniques for manipulating a single actin filament by a microneedle (Kishino & Yanagida 1988) and optical traps (Finer *et al.* 1994), and nanometry (Ishijima *et al.* 1991; Svoboda *et al.* 1993), has allowed measurement of individual mechanical events directly from single molecules of myosin or its subfragments *in vitro* (Finer *et al.* 1994; Ishijima *et al.* 1994; Mehta *et al.* 1997; Miyata *et al.* 1994; Molloy *et al.* 1995; Guilford *et al.* 1997). The displacement and force were measured by monitoring a microneedle or an optically trapped bead, attached to the end of an actin filament interacting with myosin bound to the surface of an artificial substrate. The surface was sparsely coated with myosin or its subfragments so that the actin filament would be unable to interact with more than one molecule at once. The values, however, vary widely. Some investigators have reported that the displacements of myosin are 4–6 nm (Molloy *et al.* 1995; Guilford *et al.* 1997; Mehta *et al.* 1997), consistent with the lever-arm model. On the other hand, we have reported values of 15–20 nm (Ishijima *et al.* 1996; Tanaka *et al.* 1998), which are several-fold larger than that expected from this model and suggest multiple interactions of a myosin head with actin (Harada *et al.* 1990; Higuchi & Goldman 1991; Ishijima *et al.* 1991; Lombardi *et al.* 1992; Yanagida *et al.* 1985). We have argued that the large displacement is observed when myosin molecules are under advantageous conditions, such that myosin molecules are correctly orientated relative to the actin filament, as in muscle, and dysfunction from interaction with the surface is minimized (Ishijima *et al.* 1996; Iwane

*Author for correspondence (yanagida@physl.med.osaka-u.ac.jp).

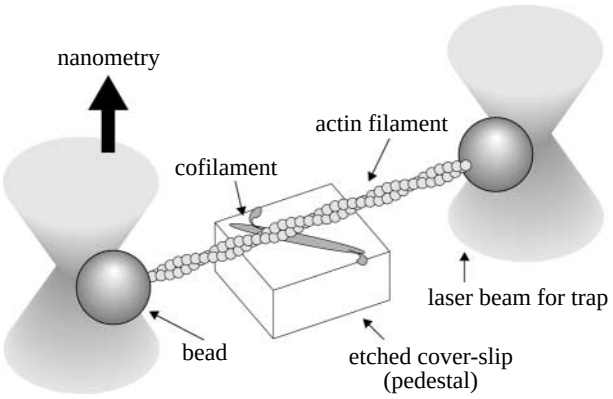

Figure 1. Schematic diagram of the measurement system of displacements of individual one-headed and two-headed myosin by optical trapping nanometry.

et al. 1997; Tanaka *et al*. 1998). It is essential to determine the displacement accurately in order to elucidate how conformational changes in the myosin head lead to force generation, and how mechanical cycles are coupled to ATP hydrolysis. Here we review our recent work in which we have made detailed measurements of myosin step size and mechanochemical coupling, and propose a model of the myosin motor.

2. DISPLACEMENTS OF ONE- AND TWO-HEADED MYOSIN

In order to measure displacements from single myosin heads, we have used one-headed myosin prepared by digesting rabbit skeletal myosin with papain. One-headed myosin was co-polymerized with myosin rod at the molar ratio of one-headed myosin to rod of 1:400 to 1:1500. An actin filament suspended by dual optical traps could be placed in contact with a myosin-rod co-filament at several different angles (figure 1*a*,*b*).

As only one to four myosin heads were distributed over a filament 5–8 μm in length and a suspended actin filament was set not to be perfectly parallel to a co-filament, the number of myosin heads which could interact with a suspended actin filament at the same time would be at most one. Figure 2*a* shows the typical time-course for the generation of displacements (i), and stiffness (ii), the latter determined by measuring variances in the fluctuations of the bead (Molloy *et al*. 1995). Figure 2*b* shows histograms of the displacements of a bead at angles of 5–10°, that is, near physiological condition. The bead displacements were widely distributed from −20 to +50 nm. The thermal fluctuations of a bead could be well fitted with a Gaussian distribution when no myosin heads interacted with the actin filament (solid line). This result is consistent with the interpretation that the large distribution is due mostly to the randomizing effect of the thermal fluctuations of the beads (Molloy *et al*. 1995). According to this interpretation, the bead mean displacement caused by a myosin head is determined by the value at the centre of the distribution, i.e. 10 nm. However, the bead displacements are usually smaller than the displacements caused by a myosin head (head displacement) because the head-induced displacement is attenuated by the system compliance (Svoboda *et al*. 1993). The mean

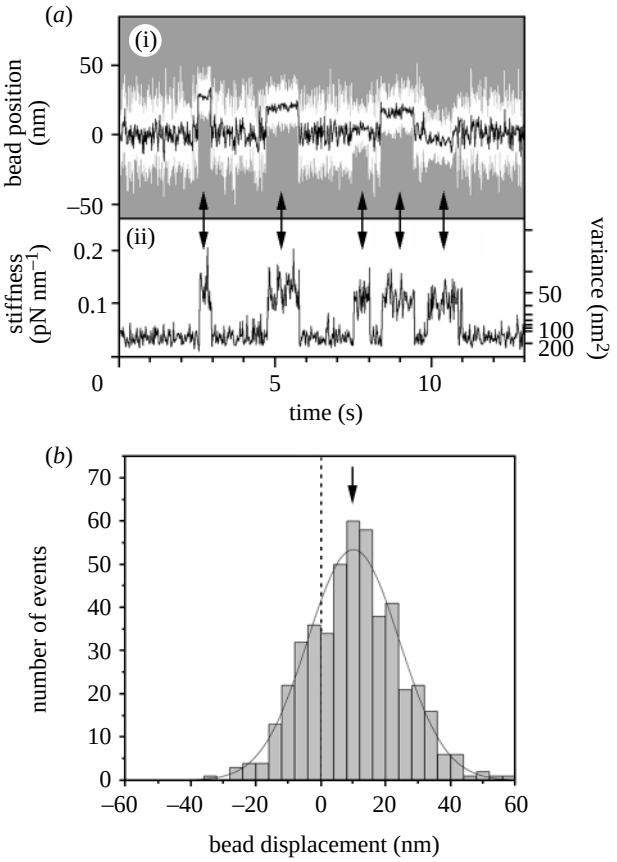

Figure 2. (*a*) (i) The time-courses of the generation of displacements by a single one-headed myosin molecule at low load. White line, raw data. Black line, same data passed through a low-pass filter of 20 Hz bandwidth. (ii) Changes in stiffness. The stiffness was obtained from the variance of the fluctuations of a bead. The concentration of ATP was 1 μM and the trap stiffness was 0.03 pN nm. Temperature, 20 °C. (*b*) A histogram of bead displacements.

head-induced displacement after correction for the compliance was 15 nm. Note that this experiment can determine only the value averaged over may displacements but cannot determine the spread of displacements of individual myosin heads, so the maximum displacement can be >15 nm.

The displacements of two-headed myosin molecules were measured similarly. Figure 3*a* shows typical time-courses for the generation of displacements (i) and the change in stiffness (ii) at the angle between an actin filament and a co-filament of 5–10°. Figure 3*b* shows a histogram of the bead displacements. The size of the mean displacement (bead displacement, 10 nm, and head displacement after correction for the compliance, 15 nm) was similar to that of one-headed myosin.

The results show that the mean displacement of a single myosin head is 15 nm near zero load and suggest that either of the two heads of a myosin molecule interact with an actin filament to produce force at low load.

3. UNITARY STEP SIZE DETERMINED BY A SCANNING PROBE METHOD

The observed mean displacement of 15 nm appears to be larger than the displacement that would be caused by a single mechanical event of a myosin head, such as a

PHILOSOPHICAL TRANSACTIONS OF THE ROYAL SOCIETY B BIOLOGICAL SCIENCES

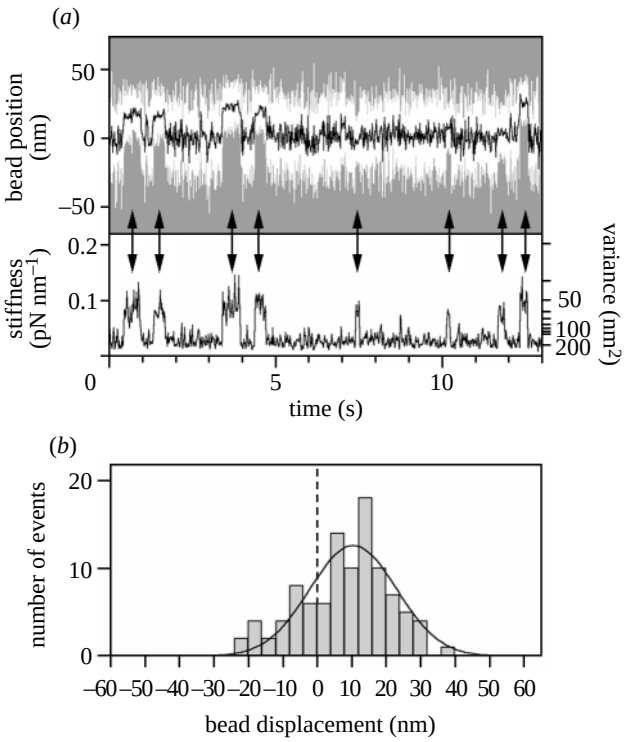

Figure 3. Displacements of two-headed myosin.

swinging motion. In order to examine whether there are substeps in the observed overall displacement, we developed a new assay to directly manipulate a single S1 molecule, which had been fluorescence labelled and visualized, and to measure its displacement with a scanning probe (Kitamura *et al*. 1999). This assay allowed us to resolve the process of the generation of displacement at high resolution, because the probe–S1–actin linkage could be greater than tenfold stiffer than the beads–actin–myosin-head linkage in the optical trap studies (Tanaka *et al*. 1998), which significantly improved the signal-to-noise ratio of the data.

A schematic diagram of the experimental arrangement is shown in figure 4*a*. S1 was biotinylated and fluorescence labelled in a molar ratio of 1:1 by exchanging its endogenous regulatory light chain by a biotinylated and fluorescence-labelled one, a subunit at the tail end on the opposite side of the ATP- and actin-binding sites. A single S1 molecule on a glass surface was specifically captured onto the tip of a scanning probe coated with streptavidin. A very sharp ZnO needle crystal ('whisker'), with a length of 5–7 μm and a radius of curvature of *ca.* 15 nm at the tip, was used as the probe. The latter was attached to a fine glass needle mounted on a three-dimensional scanner. The stiffness of the needles used was 0.01–0.02 pN nm such that the load exerted on the S1 molecule was small (<1 pN). That only a single S1 was captured was confirmed by objective-type total internal reflection fluorescence microscopy (TIRFM), which produced a clear image of single fluorophores with a high fluorescence-to-background ratio, and provided enough space for the use of a scanning probe. Figure 4*b* shows the fluorescence image of a single S1 molecule captured by the probe (marked by an arrowhead). The S1 molecule was brought into contact with an actin bundle bound to a glass surface by scanning the probe (figure 4*a*, right-hand

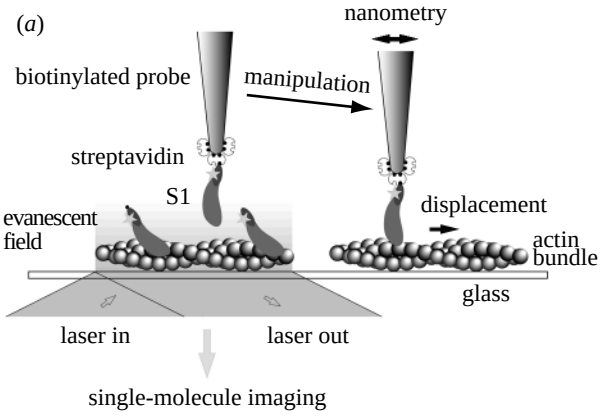

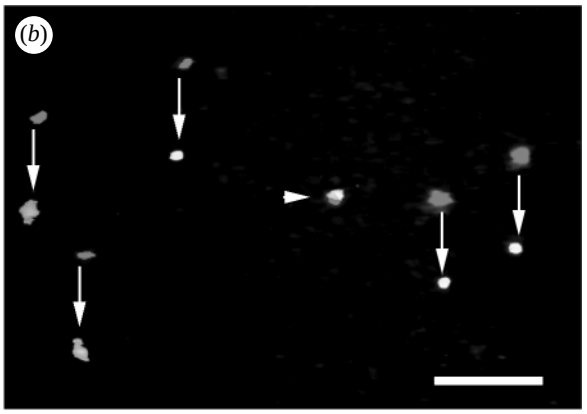

Figure 4. Direct capture and manipulation of a single S1 molecule by a scanning probe. (*a*) Schematic drawing of the experiment. A single S1 molecule, labelled with single orange fluorophores, Cy3, was specifically captured at its tail end with a scanning probe (ZnO whisker) through biotin–streptavidin and observed by the objective-type TIRFM. Displacement produced when the S1 molecule was brought into contact with an actin bundle bound to a glass surface (right-hand side) was determined by measuring the displacement of the probe with nanometre accuracy. See text for details. (*b*) Fluorescence images of single S1 molecules. The micrograph shows superimposed images of single S1 molecules captured by the probe and bound to the surface of a cover-slip when the stage was moved by a piezo scanner. The red and yellow spots represent images before and after movement, respectively. The captured S1 molecule (marked by an arrowhead) could be moved independently of the stage. Bar, 5 μm.

side). The displacements due to S1–actin interactions were determined by measuring the displacements of the needle with sub-nanometre accuracy using a split-photodiode (Ishijima *et al*. 1991).

Individual displacements due to interactions between S1 and the actin filament were detected in the presence of ATP (figure 5*a*(i)). Figure 5*a*(ii) shows corresponding changes in stiffness, which were calculated from the variance of the fluctuation of the needle. The stiffness upon binding of S1 to the actin filament (k_{S1}) was >0.5 pN nm, which was greater than tenfold larger than those by optical trapping nanometry. This is because the probe–S1–actin linkage was much more rigid. This large stiffness increased the signal-to-noise ratio at high temporal resolution and thus allowed us to observe the substeps in the rising phases of displacements as shown below. The square root-mean-square displacement of

PHILOSOPHICAL TRANSACTIONS OF THE ROYAL SOCIETY B BIOLOGICAL SCIENCES

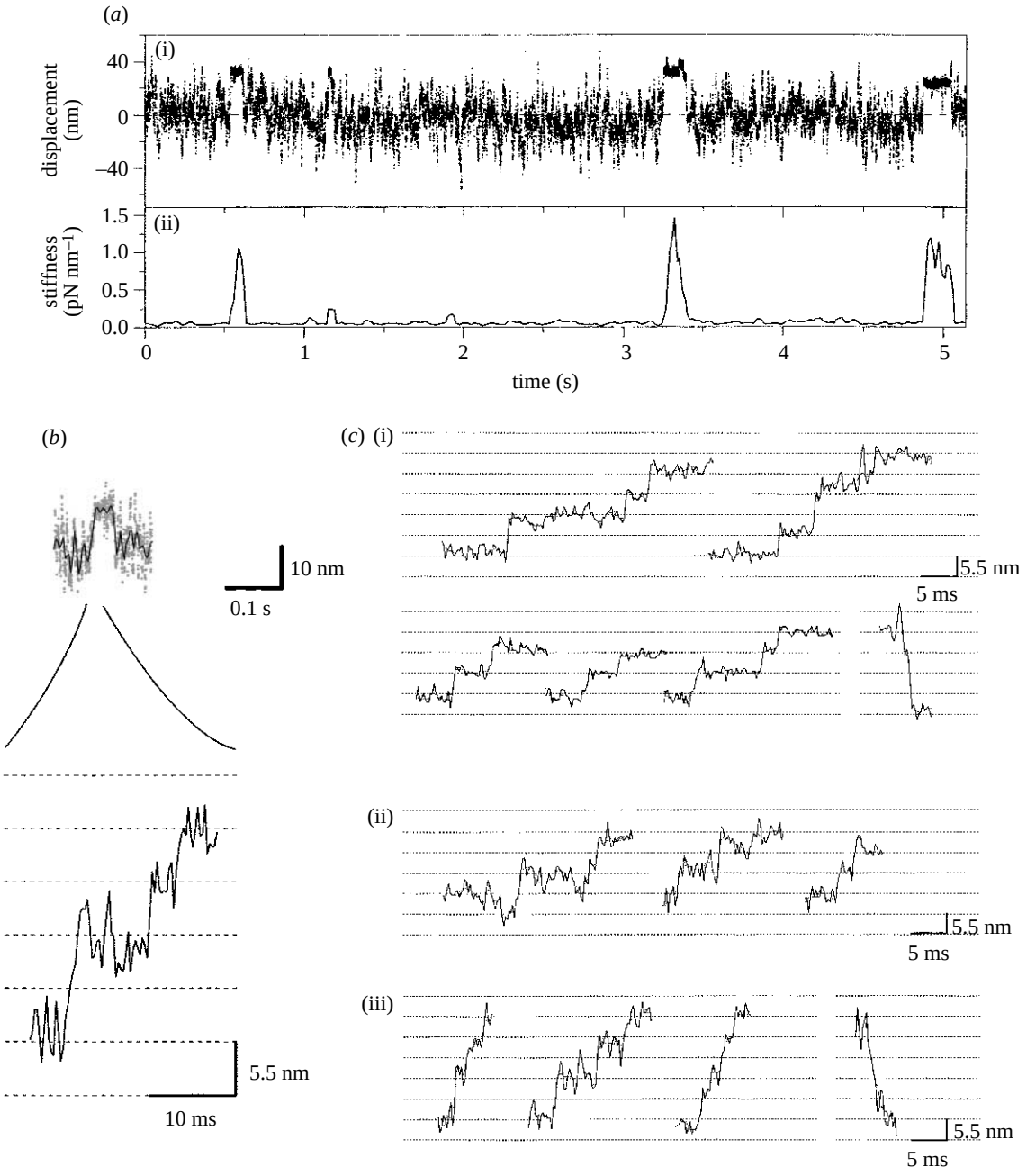

Figure 5. Displacements caused by single S1 molecules that were captured onto the tip of the scanning probe and brought into contact with an actin bundle. (*a*) A typical record of the displacements by a single S1 molecule (i) and the stiffness changes (ii). ATP concentration, 1 μM ATP; temperature, 27 ± 1 °C. (*b*) A record of the rising phase of a displacement on an expanded time-scale. (*c*) Records of the rising phases of displacements at various conditions: (i) 1 μM ATP, 20 °C; (ii) 0.1 μM ATP, 20 °C; and (iii) 1 μM ATP, 27 °C. Horizontal gridlines have been drawn at a spacing of 5.5 nm.

thermal motions of a needle decreases with the increase in k_{Sl}, according to a principle of energy equipartition, $\langle x^2\rangle^{1/2} = (k_B T/(k_{S1} + k_{needle}))^{1/2}$. As k_{Sl} is large (>0.5 pN nm), $\langle x^2\rangle^{1/2}$ decreases to <2.5 nm. In the case of optical trapping nanometry on the other hand, the total stiffness, probably due largely to the bead–actin linkage, is not larger than 0.1 pN nm at a trap stiffness of *ca.* 0.02 pN nm and hence the noise level ($\langle x^2\rangle^{1/2}$) cannot be smaller than *ca.* 6 nm. Furthermore, due to this large stiffness the displacement of Sl was attenuated little by the system compliance, that is, the observed needle displacement is equal to the head-induced displacement.

Figure 5*b* shows the rising phase of an overall displacement on an expanded time-scale. The displacement did not take place abruptly but instead developed in a stepwise fashion. Other examples are shown in figure 5*c*. Single myosin heads underwent between one and five steps to produce displacements of *ca.* 5 to *ca.* 30 nm. In order to determine whether the observed steps were regular, we used a statistical analysis that had been used for determining the step size of kinesin (Svoboda *et al.* 1993). A histogram of pairwise differences in the rise phase of displacement was computed for each record and histograms were lumped for 50 events recorded for eight different Sl molecules (figure 6*a*). The histogram shows

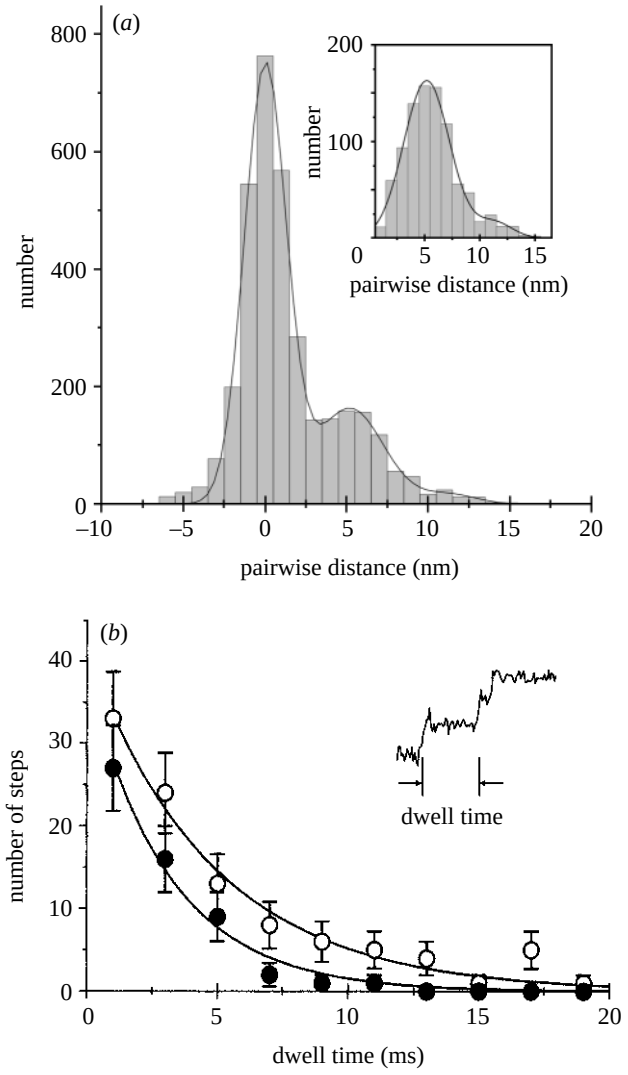

Figure 6. (*a*) Histogram of pairwise distances in the rise phase of displacements. Inset, histogram of the pairwise distances subtracting Gaussian distributions at 0. (*b*) Histograms of dwell times between steps at a concentration of ATP of 1 (filled circle) and 0.1 μM (open circle).

two peaks corresponding to the spatial periodicities of *ca.* 5.3 and *ca.* 11 nm. The spacing of the two peaks were 5.3 ± 0.2 nm (mean ± s.d.) and *ca.* 11 nm. A small shoulder was also identified near 5 nm in figure 6*a*. This shoulder may be due to backward steps. The step size was constant, and independent of the size of overall displacements, the concentration of ATP and the temperature.

The mean durations of overall displacements were 2400 and 220 ms at 0.1 and 1 mM ATP, respectively, giving second-order rate constants for ATP-induced dissociation of the actomyosin complex, *ca.* $5 \times 10^6\ M^{-1}\ s^{-1}$, consistent with values obtained for acto-Sl in solution and by optical trapping nanometry. The dwell time between steps was independent of the concentration of ATP (figure 6*b*). These results strongly indicate that each overall displacement corresponds to a single biochemical cycle of ATP hydrolysis. This conclusion agrees with simultaneous measurement of individual mechanical and ATPase events (Ishijima *et al*. 1998).

Recently, we found that substeps were also observed under load (1–3 pN). The step size (*ca.* 5.5 nm) was constant, while the number of steps and the slope of the rising phase decreased.

The results lead to the conclusion that myosin heads move along an actin filament with regular steps of 5.3 nm and undergo up to five steps to produce a maximum displacement of 30 nm during one biochemical cycle of ATP hydrolysis.

4. DISPLACEMENT OF A DELETION MUTANT OF MYOSIN WITHOUT THE LIGHT-CHAIN BINDING DOMAIN

There is a large body of evidence of conformational changes in the neck region of a myosin head in crystal, in solution and in muscle fibres (see Cooke 1997, for a review). Based on these observations, the 'tilting cross-bridge model' has been refined into the 'lever-arm hypothesis'. Although this model has been widely accepted, there has been no direct evidence that the neck region (light-chain (LC) binding domain) acts as a lever arm to produce force. To test this hypothesis, we measured displacements of single myosin molecules with and without the LC binding domain. In order to avoid the effects of damage during interaction with a glass surface and the effects of a random orientation of myosin relative to the actin filament axis, we used very sparse co-filaments of a chimera of *Dictyostelium* heavy meromyosin (HMM) with and without the LC binding domain and skeletal myosin light meromyosin (LMM). The co-filaments were 5–8 μm long and contained only a few myosin heads. An actin filament with a latex bead attached to both ends was suspended in solution by dual optical traps and brought into contact with a single myosin molecule in a co-filament fixed on a glass surface, with an angle between these filament sets of 5°. Displacement was determined by measuring the displacement of a bead with nanometre accuracy.

The mean bead displacements were 7.0 nm (14 nm after correction for the system compliance) and 6.4 nm (13 nm after correction for the system compliance) for myosin with and without the LC binding domain. The sliding velocity of an actin filament caused by many myosin molecules in a co-filament was decreased about fivefold when the LC binding domain was deleted, consistent with Uyeda *et al*. (1996).

This result suggests that the neck region does not act as a lever arm but rather regulates the kinetics of the actin–myosin interaction, and thus the velocity and direction of motion (see § 5).

5. MODEL OF THE MYOSIN MOTOR

(a) *A myosin head walks along an actin filament by Brownian motion*

The unitary step size approximately coincides with the periodicity between adjacent actin monomers in one strand of an actin filament (5.5 nm), multiple unitary steps take place during a single biochemical cycle of ATP hydrolysis and some of the steps are backwards. These results strongly indicate that a myosin head walks on actin monomers in an actin filament by Brownian motion. The myosin head, however, cannot move by hopping, because it quickly diffuses away from the actin filament while it dissociates from the actin filament.

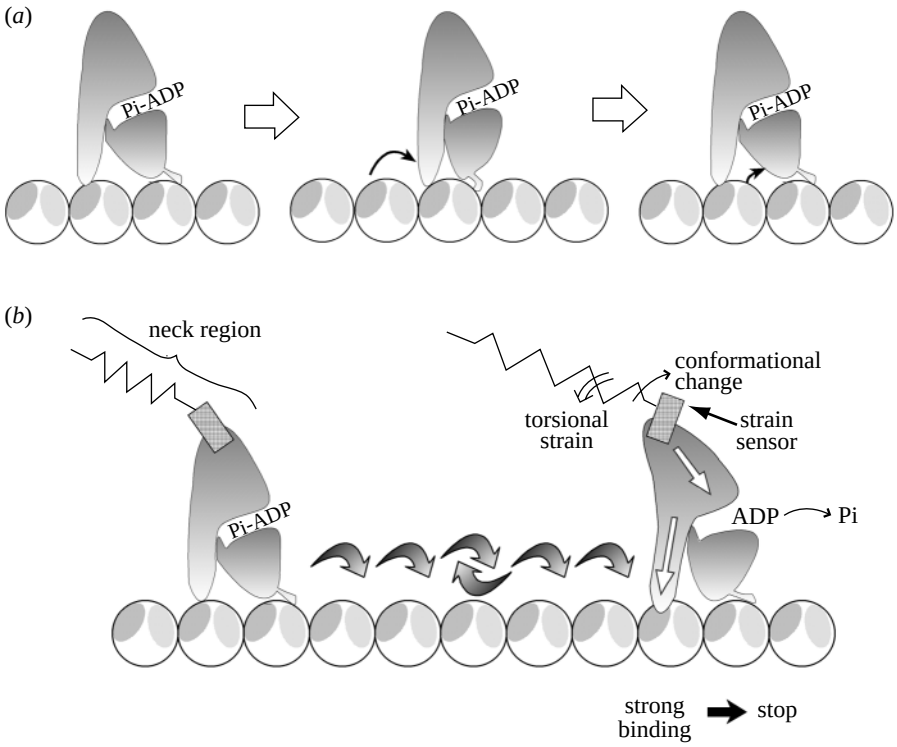

Figure 7. Model of the actomyosin motor. (*a*) A myosin head binds on its two binding sites, 50 kDa upper and lower domains, to adjacent actin monomers in rigor (Rayment *et al*. 1993*b*). A myosin head continuously 'walks' on an actin filament like an inchworm, interacting with an actin filament via these two binding sites on alternation. (*b*) The neck region acts as a strain sensor. When the myosin head steps forward along an actin filament, the neck region is torsionally strained to cause conformational change in the neck region. The conformational change accelerates the release of bound Pi from the myosin head to make the bond between actin and the myosin head rigid, and to stop the movement of the myosin head at the positive position. The motion of a myosin head along an actin filament can be purely thermal motion or thermal motion biased by the deformation of a myosin head or an actin filament (see text for detail).

A myosin head is known to bind at its major two binding sites, 50 kDa upper and lower domains, to adjacent actin monomers in rigor (Rayment *et al*. 1993*b*). The unitary step size approximately coincides with the distance between adjacent actin monomers in one strand of an actin filament (5.5 nm). Therefore, a myosin head may continuously 'walk' on an actin filament like an inchworm, interacting with an actin filament via these two binding sites on alternation (figure 7*a*). Recently, quick-frozen and rotary-shadowed electron microscopy of a myosin head moving an actin filament in the presence of ATP suggests that a myosin head makes contact with an actin filament via the 50 kDa upper and lower domains on alternation (Katayama 1998; E. Katayama, personal communication).

(b) *How is Brownian motion biased in the forward direction?*

Brownian motion is random, so it must be biased in the forward direction. We assume that the neck region plays an essential role in biasing the Brownian motion.

Conformational changes in the neck region of a myosin head indeed take place depending on the forms of nucleotide. However, myosin from which the majority of the neck region was deleted could produce displacement as large as myosin with the neck region. The neck region may regulate the kinetics of the actin–myosin interaction, and thus the direction, velocity and motion. For instance, the neck region acts as a strain sensor. When the myosin head steps forward along an actin filament, which has a helical structure, the base of the neck region, connected to the backbone through the LC binding domain, rotates around the actin filament by *ca*. 26° per step and would be torsionally strained. The torsional strain causes conformational change in the neck region. The conformational change in the neck region accelerates the release of bound Pi from the myosin head to make the bond between actin and the myosin head rigid and stop the movement of the myosin head (figure 7*b*). That is, a conformational change in the neck region causes the release of Pi, which is the reverse of the lever-arm model. Conversely, if the myosin head moves backward by thermal motion, the neck region would rotate conversely. If the reverse torsional strain is assumed to induce no conformational change in the neck region, the myosin head thermally diffuses back to the zero position without making a rigid bond with the actin. In this model, the displacement caused by a myosin head would not be proportional to the length of the neck region but the rate of mechanical reaction (step) could be greatly affected by removal of a major part of the neck region, consistent with our results.

In this model, the motion of a myosin head along an actin filament could be pure thermal motion, because the neck region acts as a strain sensor to fix the myosin head on the actin filament when the head diffuses forward along a filament. However, our experimental results have shown that the myosin head does not undergo backward steps so frequently (figure 5). The observed stepping

motion may not be pure thermal motion but thermal motion biased by, for instance, the deformation of a myosin head or an actin filament.

Figure 7 shows a proposed model based on these points.

We thank R. Cooke for valuable discussion and P. Conibear for critically reading the manuscript.

REFERENCES

Cooke, R. 1997 Actomyosin interaction in striated muscle. *Physiol. Rev.* **77**, 671–697.

Finer, J. T., Simmons, R. M. & Spudich, J. A. 1994 Single myosin molecule mechanics: piconewton forces and nanometre steps. *Nature* **368**, 113–119.

Guilford, W. H., Dupuis, D. E., Kennedy, G., Wu, J., Patlak, J. B. & Warshaw, D. M. 1997 Smooth muscle and skeletal muscle myosins produce similar unitary forces and displacements in the laser trap. *Biophys. J.* **72**, 1006–1021.

Harada, Y., Sakurada, K., Aoki, T., Thomas, D. D. & Yanagida, T. 1990 Mechanochemical coupling in actomyosin energy transduction studied by *in vitro* movement assay. *J. Mol. Biol.* **216**, 49–68.

Higuchi, H. & Goldman, Y. E. 1991 Sliding distance between actin and myosin filaments per ATP hydrolysed in skinned muscle fibres. *Nature* **352**, 352–354.

Huxley, A. F. 1957 Muscle structure and theories of contraction. *Progr. Biophys. Biophys. Chem.* **7**, 255–318.

Huxley, A. F. 1974 Muscular contraction. *J. Physiol.* (*Lond.*) **243**, 1–43.

Huxley, A. F. & Niedergerke, R. 1954 Interference microscopy of living muscle fibres. *Nature* **173**, 971–973.

Huxley, A. F. & Simmons, R. M. 1971 Proposed mechanism of force generation in striated muscle. *Nature* **233**, 533–538.

Huxley, H. E. 1969 The mechanism of muscle contraction. *Science* **164**, 1356–1366.

Huxley, H. E. & Hanson, J. 1954 Changes in the cross-striations of muscle during contraction and stretch, and their structural interpretation. *Nature* **173**, 973–976.

Ishijima, A., Doi, T., Sakurada, K. & Yanagida, T. 1991 Subpiconewton force fluctuations of actomyosin *in vitro*. *Nature* **352**, 301–306.

Ishijima, A., Harada, Y., Kojima, H., Funatsu, T., Higuchi, H. & Yanagida, T. 1994 Single-molecule analysis of the actomyosin motor using nano-manipulation. *Biochem. Biophys. Res. Commun.* **199**, 1057–1063.

Ishijima, A., Kojima, H., Higuchi, H., Harada, Y., Funatsu, T. & Yanagida, T. 1996 Multiple- and single-molecule analysis of the actomyosin motor by nanometer–piconewton manipulation with a microneedle: unitary steps and force. *Biophys. J.* **70**, 383–400.

Ishijima, A., Kojima, H., Funatsu, T., Tokunaga, M., Higuchi, H., Tanaka, H. & Yanagida, T. 1998 Simultaneous observation of individual ATPase and mechanical events by a single myosin molecule during interaction with actin. *Cell* **92**, 161–171.

Iwane, A. H., Kitamura, K., Tokunaga, M. & Yanagida, T. 1997 Myosin subfragment-1 is fully equipped with factors essential for motor function. *Biochem. Biophys. Res. Commun.* **230**, 76–80.

Kabsch, W., Mannherz, H. G., Suck, D., Pai, E. F. & Holmes, K. C. 1990 Atomic structure of the actin:DNase I complex. *Nature* **347**, 37–44.

Katayama, E. 1998 Quick-freeze deep-etch electron microscopy of the actin-heavy meromyosin complex during the *in vitro* motility assay. *J. Mol. Biol.* **278**, 349–367.

Kishino, A. & Yanagida, T. 1988 Force measurements by micromanipulation of a single actin filament by glass needles. *Nature* **334**, 74–76.

Kitamura, K., Tokunaga, M., Iwane, A. & Yanagida, T. 1999 A single myosin head moves along an actin filament with regular steps of 5.3 nanometres. *Nature* **397**, 129–134.

Lombardi, V., Piazzesi, G. & Linari, M. 1992 Rapid regeneration of the actin–myosin power contracting muscle. *Nature* **355**, 638–641.

Lymn, R. W. & Taylor, E. W. 1971 Mechanisms of adenosine triphosphate hydrolysis by actomyosin. *Biochemistry* **10**, 4617–4624.

Mehta, A. D., Finer, J. T. & Spudich, J. A. 1997 Detection of single-molecule interactions using correlated thermal diffusion. *Proc. Natl Acad. Sci. USA* **94**, 7927–7931.

Miyata, H., Hakozaki, H., Yoshikawa, H., Suzuki, N., Kinoshita Jr, K., Nishizaka, T. & Ishiwata, S. 1994 Stepwise motion of an actin filament over a small number of heavy meromyosin molecules is revealed in an *in vitro* motility assay. *J. Biochem.* **115**, 644–647.

Molloy, J. E., Burns, J. E., Kendrick-Jones, J., Tregear, R. T. & White, D. C. S. 1995*a* Movement and force produced by a single myosin head. *Nature* **378**, 209–212.

Rayment, I., Holden, H. M., Whittaker, M., Yohn, C. B., Lorentz, M., Holmes, K. C. & Milligan, R. A. 1993*a* Structure of the actin–myosin complex and its implications for muscle contraction. *Science* **261**, 58–65.

Rayment, I., Rypniewski, W. R., Schmidt-Base, K., Smith, R., Tomchick, D. R., Benning, M. M., Winkelmann, D. A., Wesenberg, G. & Holden, H. M. 1993*b* Three-dimensional structure of myosin subfragment-1: a molecular motor. *Science* **261**, 50–58.

Svoboda, K., Schmidt, C. F., Schnapp, B. J. & Block, S. M. 1993 Direct observation of kinesin stepping by optical trapping interferometry. *Nature* **365**, 721–727.

Tanaka, H., Ishijima, A., Honda, M., Saito, K. & Yanagida, T. 1998 Orientation dependent displacements by single one-headed myosin molecules in a synthetic myosin filament. *Biophys. J.* **75**, 1886–1894.

Uyeda, T. Q. P., Abramson, P. D. & Spudich, J. A. 1996 The neck region of the myosin motor domain acts as a lever arm to generate movement. *Proc. Natl Acad. Sci. USA* **93**, 4459–4464.

Yanagida, T., Arata, T. & Oosawa, F. 1985 Sliding distance of actin filament induced by a myosin cross-bridge during one ATP hydrolysis cycle. *Nature* **316**, 366–369.

Discussion

L. Cruzeiro-Hansson (*Department of Mathematics, Heriot-Watt University, Edinburgh, UK*). Could it be that the extra steps you measure are a different behaviour induced by the experimental set-up? For instance, Brownian motion in the vertical direction could generate extra strain and lead to slippage.

T. Yanagida. It could not, because the unbinding force of an actomyosin rigor complex after force generation is 9 pN, which is too large to be broken by the Brownian motion of a probe. For producing a force of 9 pN, the probe (needle) should displace by 9 pN/0.02 pN nm = 450 nm! by Brownian motion. One may misunderstand that since the probe is much larger than the S1 molecule, Brownian motion of the probe may greatly affect the motion of the S1 molecule. Note that the average energy of thermal motion is kT, independent of the size of the objects. Therefore, the energy of Brownian motion of an S1 molecule is the same as that of the probe.

PHILOSOPHICAL TRANSACTIONS OF THE ROYAL SOCIETY B BIOLOGICAL SCIENCES